

**Alexey S. Kuznetsov, Nancy J. Kopell and Charles J. Wilson**

*J Neurophysiol* 95:932-947, 2006. First published Oct 5, 2005; doi:10.1152/jn.00691.2004

**You might find this additional information useful...**

---

This article cites 69 articles, 22 of which you can access free at:

<http://jn.physiology.org/cgi/content/full/95/2/932#BIBL>

This article has been cited by 4 other HighWire hosted articles:

**Synaptic Activation of Dendritic AMPA and NMDA Receptors Generates Transient High-Frequency Firing in Substantia Nigra Dopamine Neurons In Vitro**

S. N. Blythe, J. F. Atherton and M. D. Bevan

*J Neurophysiol*, April 1, 2007; 97 (4): 2837-2850.

[Abstract] [Full Text] [PDF]

**Roles of Subthreshold Calcium Current and Sodium Current in Spontaneous Firing of Mouse Midbrain Dopamine Neurons**

M. Puopolo, E. Raviola and B. P. Bean

*J Neurosci.*, January 17, 2007; 27 (3): 645-656.

[Abstract] [Full Text] [PDF]

**An Increase in AMPA and a Decrease in SK Conductance Increase Burst Firing by Different Mechanisms in a Model of a Dopamine Neuron In Vivo**

C. C. Canavier and R. S. Landry

*J Neurophysiol*, November 1, 2006; 96 (5): 2549-2563.

[Abstract] [Full Text] [PDF]

**Modeling single-neuron dynamics and computations: a balance of detail and abstraction.**

A. V. M. Herz, T. Gollisch, C. K. Machens and D. Jaeger

*Science*, October 6, 2006; 314 (5796): 80-85.

[Abstract] [Full Text] [PDF]

Updated information and services including high-resolution figures, can be found at:

<http://jn.physiology.org/cgi/content/full/95/2/932>

Additional material and information about *Journal of Neurophysiology* can be found at:

<http://www.the-aps.org/publications/jn>

---

This information is current as of December 11, 2007 .

## Transient High-Frequency Firing in a Coupled-Oscillator Model of the Mesencephalic Dopaminergic Neuron

Alexey S. Kuznetsov,<sup>1</sup> Nancy J. Kopell,<sup>1</sup> and Charles J. Wilson<sup>2</sup>

<sup>1</sup>Center for BioDynamics and Mathematics Department, Boston University, Boston, Massachusetts; and <sup>2</sup>Cajal Neuroscience Center and Department of Biology, University of Texas at San Antonio, San Antonio, Texas

Submitted 1 July 2005; accepted in final form 28 September 2005

**Kuznetsov, Alexey S., Nancy J. Kopell, and Charles J. Wilson.**

Transient high-frequency firing in a coupled-oscillator model of the mesencephalic dopaminergic neuron. *J Neurophysiol* 95: 932–947, 2006. First published October 5, 2005; doi:10.1152/jn.00691.2004. Dopaminergic neurons of the midbrain fire spontaneously at rates <10/s and ordinarily will not exceed this range even when driven with somatic current injection. When driven at higher rates, these cells undergo spike failure through depolarization block. During spontaneous bursting of dopaminergic neurons in vivo, bursts related to reward expectation in behaving animals, and bursts generated by dendritic application of *N*-methyl-D-aspartate (NMDA) agonists, transient firing attains rates well above this range. We suggest a way such high-frequency firing may occur in response to dendritic NMDA receptor activation. We have extended the coupled oscillator model of the dopaminergic neuron, which represents the soma and dendrites as electrically coupled compartments with different natural spiking frequencies, by addition of dendritic AMPA (voltage-independent) or NMDA (voltage-dependent) synaptic conductance. Both soma and dendrites contain a simplified version of the calcium-potassium mechanism known to be the mechanism for slow spontaneous oscillation and background firing in dopaminergic cells. The compartments differ only in diameter, and this difference is responsible for the difference in natural frequencies. We show that because of its voltage dependence, NMDA receptor activation acts to amplify the effect on the soma of the high-frequency oscillation of the dendrites, which is normally too weak to exert a large influence on the overall oscillation frequency of the neuron. During the high-frequency oscillations that result, sodium inactivation in the soma is removed rapidly after each action potential by the hyperpolarizing influence of the dendritic calcium-dependent potassium current, preventing depolarization block of the spike mechanism, and allowing high-frequency spiking.

### INTRODUCTION

Mesencephalic dopamine neurons play a key role in the function of the basal ganglia and parts of the neocortex. Dopamine released by the axons of these neurons has been shown to modulate voltage-sensitive ion channels, affect the release of other neurotransmitters, alter synaptic transmission, and modulate synaptic plasticity in target areas, primarily the dorsal striatum, nucleus accumbens, and prefrontal neocortex (Centonze et al. 2003; Nicola et al. 2000). Dopaminergic neurons are autonomously active (Fujimura and Matsuda 1989; Grace and Bunney 1983b, 1984a; Harris et al. 1989; Kita et al. 1986; Lacey et al. 1987; Nedergaard and Greenfield 1992) and produce a constant background rhythmic or irregular firing pattern on which bursts may be superimposed (Celada et al.

1999; Grace and Bunney 1984b; Hyland et al. 2002; Tepper et al. 1995). Dopaminergic neurons in behaving animals have been shown to fire distinct bursts of activity, with several-fold higher rates within the burst than without, temporally locked to the reward prediction error (e.g., Schultz 2002). That is, they fire at the moment the animal receives an unpredicted reward or is unexpectedly presented with the opportunity to begin a behavioral sequence known to end with a reward. The existence of neurons that encode reward-prediction is required for one kind of learning process, called reinforcement learning, that increases the probability of re-occurrence of whatever behavior preceded success (Dayan and Ballarín 2002; Schultz 2002). Thus the shift of dopaminergic cells from background firing to burst and back is one of the few cellular events in the basal ganglia for which a clear psychological meaning has been proposed.

The mechanisms underlying the firing patterns of the dopamine neuron have been a subject of intensive study for several years. Periodic and irregular low-frequency single spiking and higher frequency burst firing are all observed in anesthetized and awake animals (Grace and Bunney 1984a; Hyland et al. 2002; Overton and Clark 1997; Tepper et al. 1995). Bursts occurring spontaneously in anesthetized animals appear similar to those seen during learning of operant tasks. In either case, firing within a burst can achieve rates of  $\geq 20$  Hz (Hyland et al. 2002; Kiyatkin and Rebec 1998; Schultz 2002). These high rates of firing are thought to be driven by synaptic activity because spontaneous bursts are not seen in slices. Bursts are probably not generated by giant long-lasting excitatory postsynaptic potentials (EPSPs) because dopaminergic cells cannot be induced to fire at rates characteristic of bursts (above  $\sim 10$  Hz) by passage of somatic current pulses (Grace and Bunney 1983a; Kita et al. 1986; Richards et al. 1997). This failure to sustain high-frequency driven firing apparently arises from a combination of powerful spike afterhyperpolarization currents that follow spike generation and spike failure with prolonged depolarization (Grace and Bunney 1983a; Richards et al. 1997). High-frequency burst firing can be observed after blockade of the calcium-dependent potassium current responsible for the postspike afterhyperpolarization (Johnson and Wu 2004; Shepard and Bunney 1991). Under these conditions, however, dopamine cells are prone to depolarization block especially during passage of depolarizing currents, and burst-like episodes of high-frequency firing are not easily elicited. Another puzzling feature of burst firing in dopaminergic neu-

Present address and address for reprint requests and other correspondence: A. Kuznetsov, Dept. of Mathematical Sciences, IUPUI, Science Bldg., LD270, 402 N. Blackford St., Indianapolis, IN 46202-3216 (E-mail: akznetsov@math.iupui.edu).

The costs of publication of this article were defrayed in part by the payment of page charges. The article must therefore be hereby marked "advertisement" in accordance with 18 U.S.C. Section 1734 solely to indicate this fact.

rons is its dependence on *N*-methyl-D-aspartate (NMDA) receptor activation. A number of studies have shown that both spontaneous bursts in vivo (see review by Overton and Clark 1997) and bursts evoked by stimulation in slices (Morikawa et al. 2003) are dependent on activation of NMDA receptors. If the burst was simply due to a large and prolonged EPSP, why would it matter whether it arose from AMPA or NMDA receptors?

Our previous models, both abstract (Medvedev and Kopell 2001), and biophysical (Medvedev et al. 2003; Wilson and Callaway 2000), have considered the firing elicited by the somatic current pulses in slices. In this situation, a frequency somewhat higher than the steady state (but much less than in spontaneous bursts) can be elicited by release of the neuron from hyperpolarization. The previous papers reproduced that behavior in models that described the neuron as a chain of oscillators where each oscillator represented the soma or a dendritic compartment. In the biophysical models, the essential currents were a voltage-dependent calcium current and a calcium-dependent potassium current, and there was also extrusion of calcium from the cell. In each compartment, the period of oscillation was determined by the filling and emptying times of the free calcium and thus depended on the ratio of surface area to volume ratio of the compartment. Hence the frequency of the uncoupled compartments depended on the diameter of the compartment, with thinner compartments having a larger natural (uncoupled) frequency, and there was a large range in uncoupled frequencies. When the coupling was strong, the coupled compartments displayed a slow periodic oscillation, like that seen in dopaminergic cells recorded in slices (Medvedev et al. 2003; Wilson and Callaway 2000). If the strength of coupling was not enough to synchronize the compartments, the model generates an irregular oscillation (Wilson and Callaway 2000), which resembles the most common firing pattern seen in vivo (Tepper et al. 1995). In our work cited in the preceding text, the models represented dynamics in a preparation in which the spikes were absent because of the addition of TTX to the bath.

In this paper, we extend our model to NMDA-evoked burst firing of the dopaminergic neurons and suggest a mechanism by which these cells can burst in response to synaptic NMDA but not AMPA activation. We also show why this would be most effective for dendritic, rather than somatic, inputs. Although there are some similarities, we distinguish the transient burst firing that we study in this paper from the rhythmic bursting that can be elicited in the presence of apamin or bath-applied NMDA (Johnson and Wu 2004; Ping and Shepard 1996) and for which different mechanisms have been proposed (Canavier 1999; Johnson et al. 1992; Li et al. 1996).

## METHODS

We start with a biophysical model similar to those in our previous work (Medvedev et al. 2003; Wilson and Callaway 2000) but add AMPA or NMDA and spike-producing ionic currents. We consider a neuron in which there is a single large somatic compartment and multiple small dendritic compartments all connected to the larger one. All compartments have the same oscillatory mechanism and spiking currents but differ in natural frequency of oscillation because of the difference in their surface area to volume ratio.

## Equations for the single compartment

We construct a spiking and a nonspiking version of each compartment in the dopaminergic cell model. Much of our work is performed using the nonspiking compartment, which was originally presented to represent the mechanisms active in the dopaminergic cell after blockade of fast spike-related currents by TTX and TEA (Wilson and Callaway 2000). The nonspiking compartment consists of a noninactivating voltage-sensitive calcium current with half-activation at about  $-20$  mV, a voltage-insensitive high-affinity calcium-dependent potassium current (half activated at 250 nM), a voltage-sensitive potassium current (half activation at  $-10$  mV), and a small leak current that limits the input resistance at very hyperpolarized potentials when all the other conductances can be zero. For simplicity, the voltage-sensitive conductances are treated as instantaneous. This has no effect on the result because the dynamics of voltage and calcium concentration are both slow relative to the activation of both of these conductances. The equations for this compartment were

$$C \frac{dv}{dt} = i_{app} + g_{Ca}(v)^4(E_{Ca} - v) + g_K(v)(E_K - v) + g_{KCa}([Ca]_i)(E_K - v) \\ + g_l(E_l - v) + g_{NMDA}(v)(E_{NMDA} - v) + g_{AMPA}(E_{AMPA} - v) \\ \frac{d[Ca]_i}{dt} = \frac{2\beta}{\tau} \left( \frac{g_{Ca}(v)}{zF} (E_{Ca} - v) - P_{Ca}[Ca]_i \right) \\ g_{KCa}([Ca]_i) = \bar{g}_{KCa} \frac{[Ca]_i^4}{[Ca]_i^4 + k^4} \\ \alpha_c(v) = -0.0032(v + 50)/(e^{-(v+50)/5} - 1) \\ \beta_c(v) = 0.05e^{-(v+55)/40} \\ g_{Ca}(v) = \bar{g}_{Ca} \{ \alpha_c(v) / [\alpha_c(v) + \beta_c(v)] \}^4 \\ g_{NMDA}(v) = \bar{g}_{NMDA} \left( 1 + \frac{[Mg]}{10} e^{-v/12.5} \right) \\ g_K(v) = \bar{g}_K / (1 + e^{-(v+10)/7})$$

Here,  $v$  is voltage,  $i_{app}$  is applied current (as a current density, in  $\mu A/cm^2$ ),  $g_{Ca}(v)$  is the voltage-sensitive calcium conductance per unit surface area (in  $ms/cm^2$ ),  $g_{KCa}$  is the calcium-dependent potassium conductance (in  $ms/cm^2$ ),  $g_l$  is the leak conductance,  $g_{NMDA}(v)$  is the voltage-sensitive NMDA conductance density, and  $g_{AMPA}$  is the AMPA conductance density. Potassium conductance was represented as a simple instantaneous sigmoidal function of voltage. The calcium conductance density was also a sigmoidal function of voltage. The AMPA conductance density was voltage-independent, but the NMDA conductance showed voltage sensitivity as in Li et al. (1996). The magnesium block of the NMDA receptor was treated as instantaneous. The reversal potentials and maximal conductances for each of the currents used in Figs. 1, 2, and 4–7 are given in Table 1.

Intracellular diffusion of calcium was not represented in the model. We have previously analyzed the effect of calcium diffusion in this model, and have shown that it does not qualitatively affect the results (Wilson and Callaway 2000). Calcium buffering was treated as

TABLE 1. Parameters for the non-spiking cell model, and the values used in Figs. 1, 2, and 7

Parameter	Value	Parameter	Value
$g_{Leak}$	0.05 mS/cm <sup>2</sup>	$E_{Ca}$	100 mV
$\bar{g}_{Ca}$	0.2 mS/cm <sup>2</sup>	$E_K$	-90 mV
$\bar{g}_K$	0.4 mS/cm <sup>2</sup>	$E_l$	-50 mV
$\bar{g}_{KCa}$	0.3 mS/cm <sup>2</sup>	$E_{AMPA}$	0 mV
[Mg]	1.4 mM	$E_{NMDA}$	0 mV
$\beta$	0.05	$P_{Ca}$	2500 $\mu m/s$

instantaneous and unsaturable. Calcium was removed from the cell by an unsaturable pump with maximum rate density  $P_{Ca}$ , and the pump was treated as nonelectrogenic. Although these simplifications are not strictly true, we verified in simulations that they did not alter the overall outcome of the model, and they greatly simplified the analysis. Calcium entering through the NMDA channel was assumed to be small compared with that entering via the calcium channel itself, and was not included in the calcium equation, in which  $\beta$  is the ratio of free to total calcium,  $r$  is the radius of the compartment (in  $\mu\text{m}$ ),  $z$  is the valence of calcium, and  $F$  is Faraday's constant.

### Two-compartment model

All compartments were given a length of  $1 \mu\text{m}$ . This has no effect on the solutions for the single compartment in which all currents are expressed as densities anyway (membrane capacitance  $C$  was  $1 \mu\text{F}/\text{cm}^2$ ). For the coupled compartment model, absolute length is still unimportant, but adjustments of the relative length of the dendritic and somatic compartments effectively adjust the ratio of dendritic to somatic surface area, and hence the strength of the dendritic contribution to the coupled oscillation. This occurs because the compartments are all treated as isopotential, and any increase in length only alters the total surface area of the compartment without affecting its surface area to volume ratio. This is inaccurate of course because distribution of charge along long dendrites is slow enough to generate voltage gradients along the dendrite that would complicate the result. Because we wanted to study the interaction between compartments without these complications, we left the compartment lengths constant and adjusted the dendritic to somatic surface area ratio by adjusting the number ( $n_d$ ) of identical synchronous dendritic compartments attached to the soma. Because we assumed all dendrites were synchronous, attaching  $n_d$  isopotential dendritic compartments to the soma is the same as attaching a single isopotential compartment with an  $n_d$ -fold increase in surface area.

Compartments were coupled by voltage. There was no diffusion of calcium between compartments. The strength of the electrical coupling between the somatic and dendritic compartments is an important issue for models of this type. Because the dendritic membrane is represented by a single compartment, the most realistic strength of coupling to use cannot be computed from the cytoplasmic resistivity as done in cable models (Li et al. 1996). We tried a variety of values for the coupling parameter for the pair of compartments  $g_c$ , but the results shown here were obtained with values ranging from 0.25 to 0.30  $\text{mS}/\mu\text{m}$ . In a previous work, we considered the case in which coupling was very strong, and the entire cell was effectively isopotential (Medvedev et al. 2003), as likely is effectively the case during spontaneous oscillations in the absence of spiking (Wilson and Callaway 2000). Distributed models of the dopaminergic neuron suggest that under some conditions, substantial voltage differences exist along the dendritic membrane (Wilson and Callaway 2000), and these are likely to be especially pronounced during action potential generation. Here we required that the coupling be moderately strong so that steady-state voltage gradients were small, but large voltage gradients were possible during transients. This level of coupling approximates that seen in the most realistic distributed models currently available (Canavier et al. 1999; Wilson and Callaway 2000). The current balance equations governing each of the two compartments in the coupled model were

$$C \frac{dv_d}{dt} = \sum g_{\text{ion}}(v_d - V_{\text{ion}}) + g_c \frac{r_d^2 r_s}{l_d(l_d l_d^2 + l_s r_s^2)} (v_d - v_s)$$

$$C \frac{dv_s}{dt} = \sum g_{\text{ion}}(v_s - V_{\text{ion}}) + n_d g_c \frac{r_d r_s}{l_s(l_s r_s^2 + l_d r_d^2)} (v_s - v_d)$$

in which  $v_d$  and  $v_s$  are the dendritic and somatic voltages,  $l_d$  and  $l_s$  are dendritic and somatic lengths (always  $1 \mu\text{m}$ ), and  $r_d$  and  $r_s$  are the dendritic and somatic radii.

### Spiking model

To the preceding model, we added spike-producing sodium and potassium conductances to each compartment. Specifically

$$\alpha_m(v) = -0.32(v + 31)/(e^{-(v+31)/4} - 1)$$

$$\beta_m(v) = -0.28(v + 4)/(e^{v+4}/5 - 1)$$

$$m_\infty(v) = \alpha_m(v)/[\alpha_m(v) + \beta_m(v)]$$

$$\alpha_h(v) = 0.01 e^{-(v+47)/18}$$

$$\beta_h(v) = 1.25/(1 + e^{-(v+24)/5})$$

$$\frac{dh}{dt} = \alpha_h(v)(1 - h) - h\beta_h(v)$$

$$g_{\text{Na}}(v, h) = \bar{g}_{\text{Na}} m_\infty(v)^3 h$$

$$\alpha_n(v) = -0.0032(v + 5)/(e^{-(v+5)/10} - 1)$$

$$\beta_n(v) = 0.05 e^{-(v+10)/16}$$

$$\frac{dn}{dt} = \alpha_n(v)(1 - n) + n\beta_n(v)$$

$$g_{\text{KS}}(n) = \bar{g}_{\text{KS}} n^4$$

in which  $h$  is the sodium inactivation variable, and  $n$  is the activation variable for the delayed rectifier. The simplifications introduced by making the activation of voltage-dependent calcium and sodium currents instantaneous did not affect the outcome because both of these are fast, and the relative speeds of the two currents was not very important for the dopamine cell model, in which most calcium entry occurred as a result of subthreshold oscillations rather than as a spike-triggered tail current. This was verified by comparing the results to an otherwise identical model with more accurate sodium and calcium kinetics. The spike-triggered (delayed rectifier) potassium current was added to the spiking model without removing the smaller instantaneous potassium current with a more negative activation that was used in the nonspiking model. The additional parameters used in the spiking version of the model, were  $\bar{g}_{\text{Na}}$ , which was set at 150  $\text{mS}/\text{cm}^2$  and  $\bar{g}_{\text{KS}}$ , which was 4  $\text{mS}/\text{cm}^2$ . Computer simulations were performed using XPPAUT (Ermentrout 2002) using the stiff method and a time step of 0.1 ms.

## RESULTS

### Slow spontaneous oscillation in a single compartment

Our approach is based on the coupled oscillator model for the dopaminergic neuron (Medvedev et al. 2003; Wilson and Callaway 2000). That reduced model did not address action potential generation but only the subthreshold oscillations observed after blockade of sodium currents by treatment of the cells with TTX. The fundamental features of this model are illustrated for a single compartment in Fig. 1. The depolarizing phase of the membrane potential oscillation occurred when intracellular calcium concentration and calcium-dependent potassium current were low, the voltage-sensitive calcium conductance was activated, and calcium influx exceeded efflux. When the resulting increase in calcium concentration and increase in calcium-dependent potassium conductance achieved a sufficient level that calcium-dependent potassium current exceeded the calcium current, the model hyperpolarized regeneratively and stayed hyperpolarized until calcium levels were reduced by the plasma membrane calcium pump. Calcium concentration lagged calcium current because of the

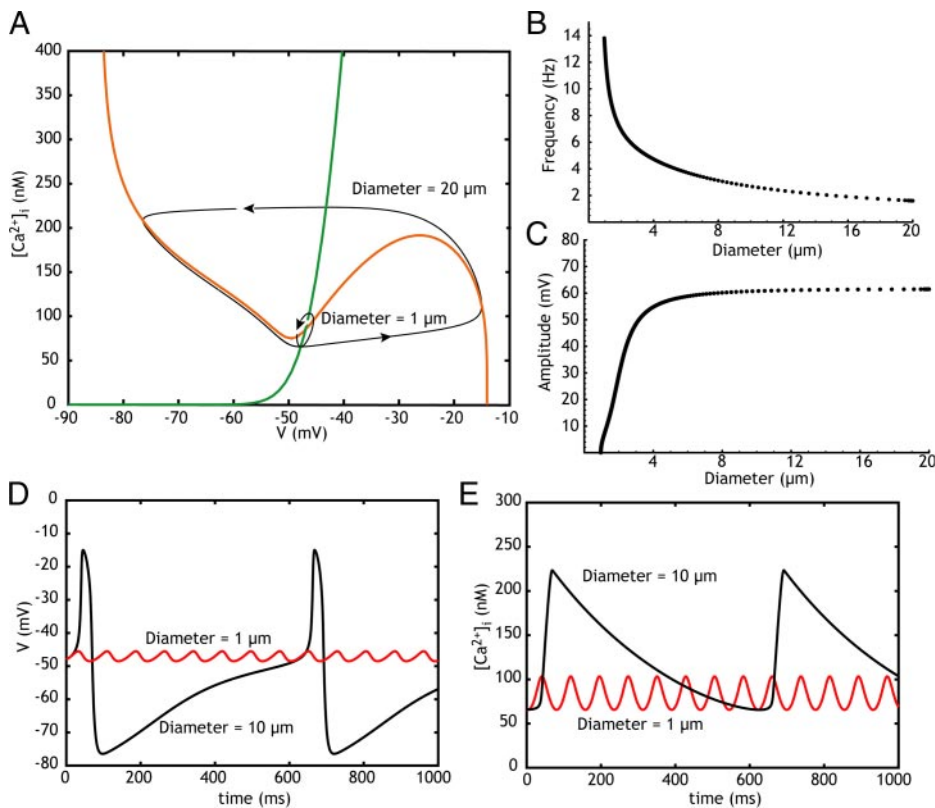


FIG. 1. Dependence of frequency and amplitude of oscillations on diameter in the isolated compartment. *A*: locations of nullclines does not depend on diameter, but the frequency is determined largely by the surface area to volume ratio, which decreases with diameter. At very low diameters, the phase trajectory deviates from the usual relaxation oscillator pattern because at very high frequencies, the membrane time constant limits the rate at which the voltage can change. *B*: relationship between frequency and diameter for the single compartment dopamine cell model. Note that for compartments of diameter comparable to the soma, the resting frequency is near 2 Hz, and for a 1- $\mu$ m dendrite, it is maximal near 14 Hz. *C*: amplitude of the oscillation decreases dramatically for fine dendrite-sized compartments, and the oscillation fails near 1  $\mu$ m. *D* and *E*: voltage and calcium concentration oscillations respectively for the 10- and 1- $\mu$ m-diam compartment

time required to fill the volume of the compartment, and likewise the time required for calcium removal was dependent on the volume. Both calcium influx and efflux depended on the membrane surface area, so the frequency of the oscillation was related to the surface area to volume ratio of the compartment. Although not essential for the oscillation, the voltage-sensitive potassium current was required to prevent large amplitude calcium spikes in the model. This is consistent with the observation of large-amplitude calcium spikes in real dopaminergic cells after treatment with high doses of TEA (e.g., Grace and Onn 1989).

This highly reduced model for the dopaminergic neuron omits a number of known features of these cells. For example, there are a number of different calcium currents that have been identified in dopaminergic neurons (Durante et al. 2004; Nedergaard et al. 1993; Wolfart and Roeper 2002), and these have all been subsumed into a single current in the model. Likewise, a variety of voltage-sensitive potassium currents are represented by a single current, the current generated by the calcium pump is disregarded, and the dynamics of calcium diffusion are not included. The kinetics of activation and deactivation of the calcium and potassium conductances are fast compared with the time course of changes in membrane potential, and these currents are treated as instantaneous. We do not include a variety of ion channels known to be present in the dopaminergic cell but that play a modulatory role in the oscillation (e.g., Neuhoff et al. 2002). Although these simplifications alter the size and shape of the oscillations somewhat, the dependence of the oscillation frequency of any cell process on its diameter is maintained (Wilson and Callaway 2000). The chief advantage of the reduced model is the ability to represent it in a two-dimensional phase plane as shown in Fig. 1. As pointed out

previously (Medvedev et al. 2003; Wilson and Callaway 2000), the positions of the nullclines in this simplified model, and hence the position of the equilibrium point at their intersection do not depend on diameter. For those sets of parameters at which the model exhibits membrane potential oscillations, the surface area to volume ratio, and hence the diameter, primarily determines the period of oscillation. For very small diameters, (e.g., 1  $\mu$ m as shown in Fig. 1), the waveform of oscillation does depend on diameter. But for a wide range of diameters that yield low oscillation frequencies, the oscillation operates in the relaxation mode in which calcium concentration changes much more slowly than the membrane potential, and the trajectory remains close to the voltage nullcline except at the rapid voltage changes that occur at the minimum and maximum values of calcium concentration. Over this range of diameters, the amplitude of the oscillation does not depend on diameter. Calcium concentration changes more rapidly in the small-diameter dendrites, but the voltage rate of change is not increased. This increase in calcium rate of change reduces the difference in time scales between voltage and calcium concentration, and the trajectory leaves the vicinity of the voltage nullcline. At these frequencies, the oscillation is smaller in amplitude, in both the voltage and calcium directions (Fig. 1). For very-small-diameter dendrites, the oscillation fails completely, despite the absence of any change in the intersection of the nullclines, as the rates of change of voltage and calcium concentration become comparable.

#### Oscillations in the coupled two-compartment system

Wilson and Callaway (2000) showed that the currents responsible for this oscillation exist on both the soma and the

dendrites of dopamine neurons. These neurons possess a sparsely branched dendritic tree consisting mostly of long segments of dendrite on the order of  $1\ \mu\text{m}$  in diameter, connected to a soma of diameter  $15\text{--}25\ \mu\text{m}$  by some short large-diameter primary dendrites (Juraska et al. 1977; Tepper et al. 1987; Wilson and Callaway 2000). It was proposed that the different regions of the neuron should tend to oscillate at different frequencies and that the resulting oscillation would occur at a frequency higher than the natural (uncoupled) frequency of the soma but lower than that of the dendrites. Wilson and Callaway (2000) further showed that under resting conditions, the dendrites and soma oscillate at a frequency corresponding approximately to the somatic natural frequency. This is expected if the various parts of the cell are strongly coupled by voltage (i.e., if the cytoplasmic resistance between soma and dendrites is low) (Medvedev and Kopell 2001; Medvedev et al. 2003) and if the amplitude of dendritic oscillations is lower than that of the soma.

The effect of dendritic diameter on the peak-to-peak amplitude and frequency of the coupled system is shown in Fig. 2. Reducing the diameter of one compartment relative to the other will increase the frequency of the pair, but this effect is small and does not continue over the entire range of diameters. The ability of a high-frequency small compartment to influence

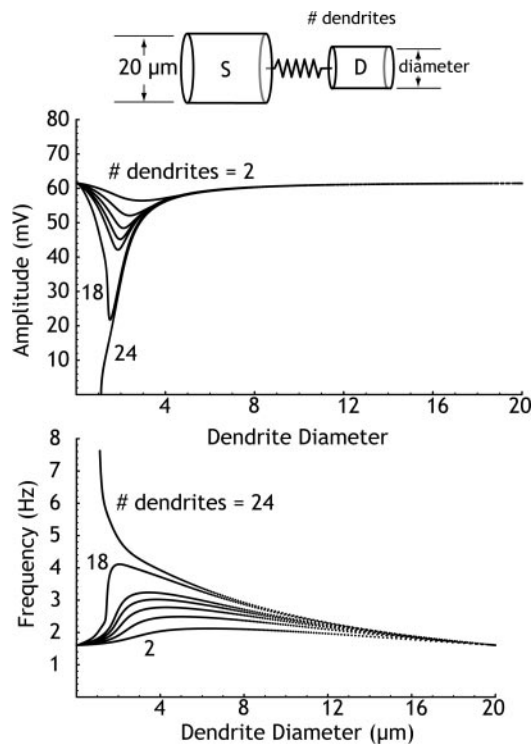


FIG. 2. Effect of diameter of a set of small compartments (D) coupled to a single larger one of constant diameter (S, diameter =  $20\ \mu\text{m}$ ). All dendrites are assumed to be identical and synchronized and so are represented by a single compartment. The influence of the dendritic compartment on the somatic one is increased with addition of extra dendritic compartments. When the number of dendrites is low, the frequency and amplitude of the oscillation of the coupled system is only slightly affected by decreases in the diameter of the dendrite (number of dendrites = 2). The overall frequency and amplitude are approximately that for the larger compartment. With larger numbers of dendrites, the coupled system can achieve higher frequencies, ultimately achieving the high natural frequency and the low-amplitude characteristic of the fine dendritic compartment (as in Fig. 1)

the coupled pair is limited by the smaller current generated by the reduced surface area of a smaller compartment. Thus as the smaller compartment is reduced in diameter below about half the diameter of the larger one, the influence of the dendrite is reduced and frequency decreases and finally becomes equal to that of the large compartment alone. This result can be altered by increasing the dendritic surface area, by either making the dendrites longer or increasing the number of dendrites. Increasing dendritic length is complicated by issues of charge transfer along the longitudinal resistance of the dendrite, so in Fig. 2 we illustrate the effect by altering the number of dendritic compartments. As the number of small dendritic compartments attached to the single large somatic compartment is increased, the maximum oscillation frequency increases, and the dendritic diameter that is optimal for generating a high-frequency oscillation decreases. However, the amplitude of the oscillation also decreases with decreasing diameter and increasing frequency of oscillation, as shown in Fig. 1. For the value of membrane capacitance and leak conductance used in all figures presented here ( $1\ \mu\text{F}/\text{cm}^2$  and  $0.05\ \text{mS}/\text{cm}^2$ ), the passive time constant was  $20\ \text{ms}$ , which is close to that observed in dopaminergic neurons, and of course this was independent of diameter. Altering the time constant by adjusting the leak conductance could not overcome the upper limit on the frequency of the coupled system ( $\sim 10\ \text{Hz}$ ) because increases in leak conductance decreased the amplitude of the oscillation and decreases in the leak conductance lowered its frequency. Like dopaminergic neurons oscillating spontaneously in slices, this two-compartment model is restricted to a frequency range between  $0$  and  $\sim 10\ \text{Hz}$ . In this mode of firing, dopaminergic cells fire one action potential on every cycle of the oscillation, and calcium levels during the course of the oscillation are not much affected by the presence or absence of action potentials (Wilson and Callaway 2000). The pattern of firing is determined entirely by the subthreshold oscillation.

#### Addition of action potential currents

In the absence of biophysical data on the action potential currents of dopaminergic cells, the choices concerning the properties of spiking currents to be added were based on known features of the overall spiking activity of dopamine cells. If the spiking currents were adjusted so that the cell could fire repetitively at high rates in response to powerful depolarizations like those seen after depolarization block of the slow oscillation, then the model would exhibit high-frequency firing independently of the slow oscillation, whenever high values of current were applied. This outcome was incompatible with the observation that dopaminergic neurons do not fire at high rates in response to injected current, so spiking mechanisms of this class were excluded. One way to limit the maximum rate of evoked spiking to that seen in dopaminergic cells was to include powerful long-lasting voltage-sensitive potassium currents triggered by action potentials. This was ruled out on the basis of reports that most single-spike afterhyperpolarization by dopaminergic cells is sensitive to apamin, a blocker of the calcium-dependent potassium current responsible for the subthreshold oscillation (Nedergaard 2004; Ping and Shepard 1996; Shepard and Bunney 1991).

For the spiking compartment models presented here, spike frequency during the slow oscillations and during current injection was limited by voltage-dependent sodium channel inactivation. There is ample indirect evidence of failure of somatic action potentials because of depolarization block. For example, the initial segment-somatodendritic (IS-SD) delay for spontaneous action potentials is increased, and finally the somatodendritic spike is blocked, by small constant somatic depolarizations (Grace 1983a,b). To maintain the simplicity of the model, this was implemented by adjusting the voltage sensitivity of activation of the potassium conductance, and the time constant and voltage sensitivity of inactivation of the spike-generating sodium channels. Most importantly, the voltage sensitivity of the potassium channel that repolarized the action potential was set so that it deactivated at a more positive voltage than required for removal of sodium inactivation (half-activation at about +20 mV). This ensured that the spike repolarizing current generated by an action potential was not by itself sufficient to remove sodium channel inactivation generated because of that action potential. Thus the action currents would not by themselves support repetitive firing in response to constant current. The voltage sensitivity of inactivation was adjusted so that >90% of sodium channels were available at -45 mV and about half of sodium channels were inactivated at -35 mV. Sodium channel activation was instantaneous and the channel was half activated at -10 mV. This resulted in a small and narrow window conductance (0.025% of maximum) centered at -35 mV. Because sodium channel density was set high (usually 150 mS/cm<sup>2</sup>), this window conductance produced a noninactivating inward current that contributed to the slow oscillation. These choices were not meant to represent accurately the biophysical properties of the

dopaminergic cell but to recreate its most fundamental firing properties with the minimal number of additional variables.

When spiking compartments of two different sizes were connected, the net oscillation was slightly higher frequency than that observed for the same compartments without sodium action potentials. The interaction between two spiking compartments was more complex than that for the nonspiking model, but it was basically similar. An example is shown in Fig. 3, in which a compartment representing 10 synchronous spiking dendritic segments of 1  $\mu$ m diameter are connected to a 20- $\mu$ m-diam soma. Spiking is nearly synchronous (Fig. 3A), but the membrane potential in the soma and dendrites are different throughout most of the cycle, and there are substantial currents flowing between compartments (Fig. 3B). Action potentials begin in the somatic compartment, but spike repolarization is more rapid in the dendrite because of the large calcium concentration transient, which produces a large rapid potassium current that is not present in the somatic compartment. A substantial proportion of the somatic repolarization that occurs after a single action potential in this model arises from the dendritic compartment. This can be seen in the longitudinal current that passes between the two compartments, shown in Fig. 3B. During the ramp-like depolarization that leads to the next action potential, the dendrite is prevented from oscillating by hyperpolarizing current from the soma, which is seen as negative in Fig. 3B. This can also be seen in the phase plane in Fig. 3D by the fact that the dendrite's trajectory follows the calcium nullcline during this portion of the cycle. The difference in membrane potential between the two compartments, and the inter-compartmental currents that result, cause each compartment to distort the phase plane of the other. In Fig. 3D, the voltage nullcline is shown for a point at

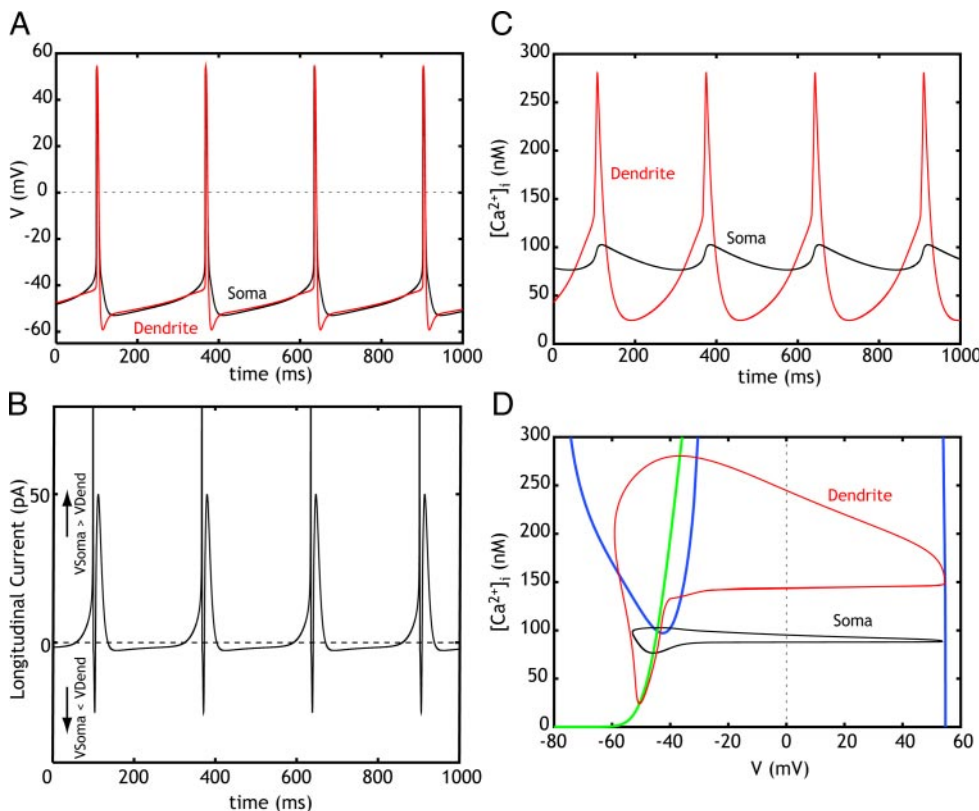


FIG. 3. Oscillations of a 2-compartment spiking model, with number of dendrites = 10, dendritic diameter of 1  $\mu$ m, and somatic diameter of 20  $\mu$ m. *A*: voltage oscillations in the soma and dendrites. Note the oscillation frequency is only slightly faster than the nonspiking model (see Fig. 1). The oscillation frequency is primarily determined by the somatic compartment. *B*: current passing between the soma and dendrite during the oscillation. Upward indicates current flow from soma to dendrite, downward deflections means that the dendrite is more depolarized than the soma. Note the large component of spike afterhyperpolarization current contributed by the dendrite, but the soma is depolarizing the dendrite through most of the slow ramp period between spikes. *C*: calcium concentration in the soma and dendrite. Note large calcium transients in the dendrite that are responsible for the fast hyperpolarizing influence of the dendrites. *D*: phase plane representation of the dendritic and somatic voltage and calcium trajectories. The blue line is the voltage nullcline for both compartments, calculated at their isopotential point preceding each spike. The green line is their shared preceding calcium nullcline. During the ramp preceding spiking, the dendrite is effectively passive, and its trajectory follows the calcium nullcline.

which the soma and dendrites are at the same voltage. During the oscillatory cycle, the voltage nullcline of each compartment shifts over a wide range, reflecting the effect of longitudinal current flowing between compartments.

Applying current to the somatic compartment of this model cannot drive the model to fire at rates faster than that observed for the nonspiking model. This limit exists because repolarization of the somatic membrane relies on calcium-dependent potassium current that arises from the calcium-driven oscillation. To clarify why injected current cannot drive the cell to higher frequencies, effects of current and synaptic input to the nonspiking model will be described first, and the spiking model will be revisited afterward.

#### Current injection or synaptic activation of the single compartment

Injection of somatic current in the dopaminergic neuron cannot drive the cell at rates much above 10 Hz, even transiently (e.g., Richards et al. 1997). Figure 4 illustrates the effect of current application on the calcium-driven oscillation in a single nonspiking compartment. Injecting current increases the frequency of oscillation, but the amplitude of the oscillation is also decreased, and the oscillation rapidly fails. This failure occurs because of a block of the calcium oscillation that occurs when the calcium-dependent potassium current can no longer

exceed that of the combined calcium current and injected current. Block occurs when the intersection of the voltage and calcium nullclines becomes a stable equilibrium for the cell. Stability cannot be assessed simply from examination of the slope of the voltage nullcline at the intersection because, for small diameters, the oscillation deviates from the relaxation mode of operation as described earlier. This makes block of the oscillation diameter-dependent. In Fig. 4, for example, the 1- $\mu\text{m}$ -diam dendrite has ceased oscillating with injected currents above  $\sim 4 \mu\text{A}/\text{cm}^2$ , whereas the 20- $\mu\text{m}$  one continues to oscillate at higher current injections, albeit with small amplitude.

Synaptic activation of the dopaminergic neuron's dendrites can generate a burst of firing at rates that exceed the 10-Hz limit seen for the spontaneous oscillation. This response is dependent on activation of NMDA receptors and can also be evoked by dendritic application of NMDA (Morikawa et al. 2003). A comparison of the effects of NMDA and of AMPA on the calcium oscillation in the single-compartment model is shown in Fig. 5. AMPA receptor activation has an effect similar to current injection in that it raises the voltage nullcline. But because of its positive reversal potential, the effects of AMPA activation are most pronounced in the hyperpolarizing phase of the oscillation, for which the driving force for AMPA-mediated current is greater. This causes the oscillation to undergo a powerful reduction in amplitude, and then to fail in the soma-sized compartment at frequencies  $< 10$  Hz. For a smaller compartment, the oscillation frequency can achieve much higher frequencies, but the amplitude is very small at all frequencies.

Because of its voltage dependence, the NMDA receptor undergoes voltage-dependent block and unblock on each cycle of the oscillation. While NMDA activation is slow, the voltage-dependent block of the receptor is rapid (Mayer and Westbrook 1985). Because it is mostly blocked during the hyperpolarizing phase of the oscillation, activation of the NMDA receptor has much less effect on the phase plane and voltage trajectory in the hyperpolarizing phase but primarily influences the depolarizing phase of the oscillation. This voltage sensitivity can be seen in the voltage nullcline. Thus NMDA receptor activation increases the amplitude of the oscillation for all diameter compartments. Increasing NMDA receptor activation first increases frequency moderately and then at higher levels decreases frequency. The increased rate of change of voltage in both the hyperpolarizing and depolarizing directions produced by the extra voltage-dependent current through the NMDA channel causes the change in the voltage nullcline, allowing the oscillation to survive in finer dendritic processes (compare with Fig. 1B). At very high levels of NMDA conductance, oscillation frequency decreases, and larger calcium-dependent potassium currents become required to repolarize the cell in opposition to the combined depolarizing influence of inward calcium current and NMDA current. With still higher NMDA conductance, the cell would exhibit slow plateau potentials dominated by the NMDA current (not shown). In Fig. 5, all current carried by the NMDA receptor is sodium. The oscillation frequency would be increased somewhat if a portion of the current were carried by calcium, as in natural NMDA receptors, because it would increase the rate of calcium filling of the compartment.

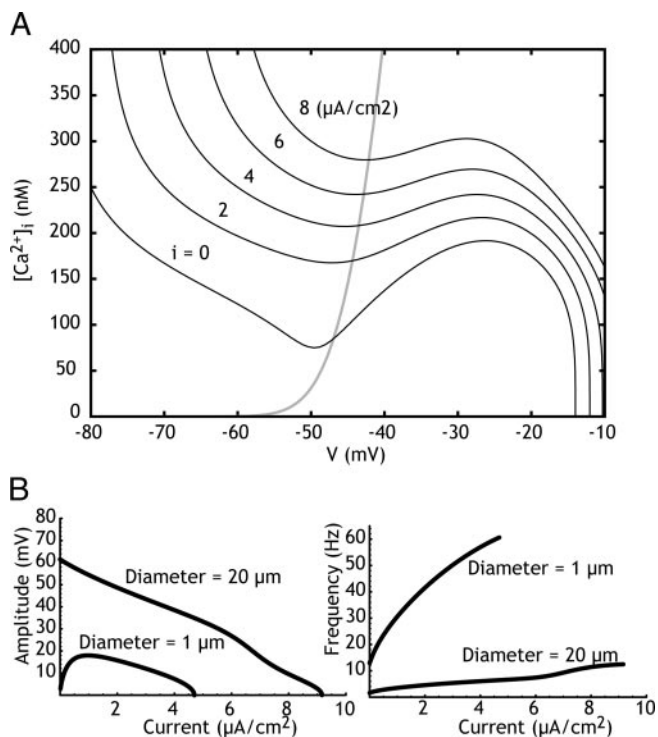


FIG. 4. Effects of applied current on the single oscillatory (nonspiking) compartment model. *A*: applied current acts on the voltage nullcline (black), raising it but also reducing the amplitude of the oscillation both in voltage and calcium. The calcium nullcline (gray) is not changed. *B*: effect on frequency is much greater for smaller diameter processes. For a 20- $\mu\text{m}$  soma, stability of the oscillation is lost by depolarization block at a maximum frequency of  $\sim 12$  Hz. For a 1- $\mu\text{m}$  dendrite, the frequency range can extend as high as 50 Hz and would go higher except that stability of the oscillation is lost at lower current levels (at  $\sim 4.7 \mu\text{A}/\text{cm}^2$ ). The amplitude of the oscillation for the small dendrite becomes increasingly small at frequencies  $> 25$  Hz, reducing its potential for influencing the soma in the coupled model.



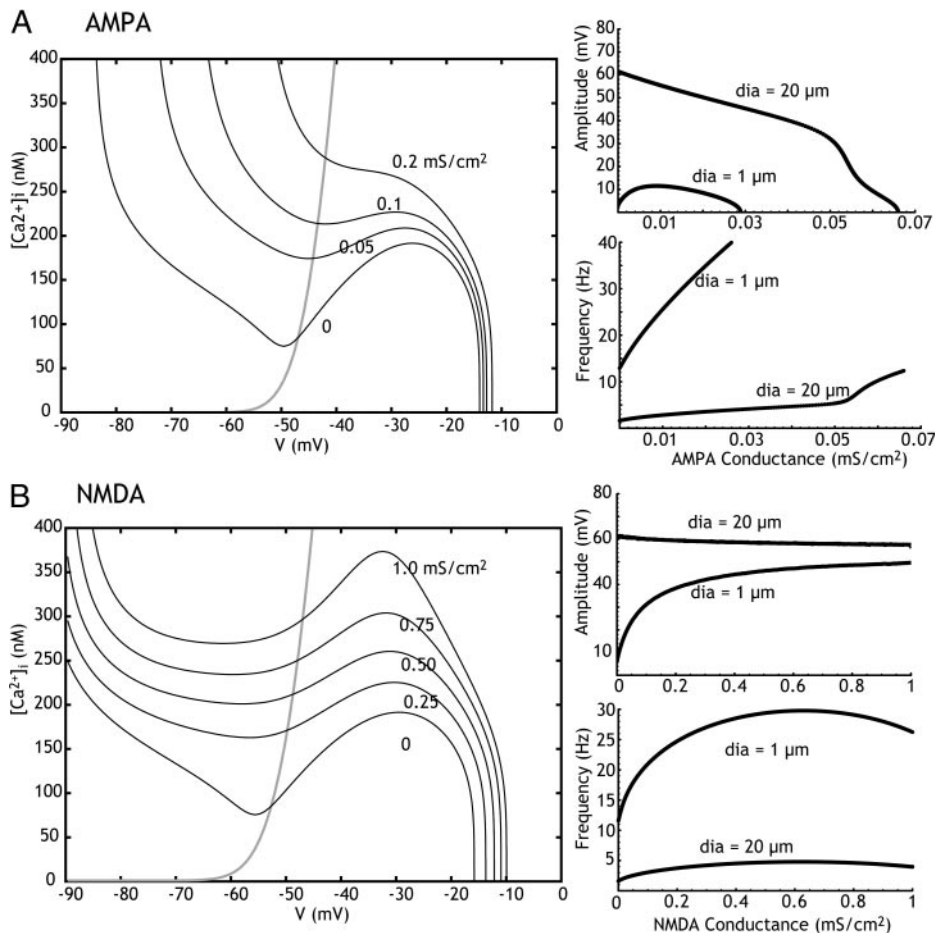


FIG. 5. The effects of AMPA and *N*-methyl-D-aspartate (NMDA) activation on the properties of the single-compartment model. *A*: AMPA activation is similar to current injection, raising and distorting the voltage nullcline (black). The calcium nullcline (gray) is not changed. High-frequency oscillations cannot be evoked in large diameter compartments by AMPA receptor activation. Small-diameter dendrites can oscillate at high-frequency, but those oscillations have very low amplitudes. At high levels of AMPA activation (near 0.07 mS/cm<sup>2</sup> in this example), oscillations cease, as they do for injected current. *B*: NMDA activation has a very different effect on the oscillation due to its voltage sensitivity. This difference is especially evident from the effect on the voltage nullcline. As a result, NMDA receptor activation increases the amplitude of oscillations, and has a moderate and biphasic effect on the frequency. NMDA does not produce depolarization block in the activation range illustrated.

#### Two compartments, with synaptic activation restricted to the dendrite

The effect of AMPA receptor activation restricted to a set of 10 1- $\mu$ m dendritic compartments attached to a single 20- $\mu$ m soma is shown in Fig. 6. In the single-compartment case, we saw that AMPA conductances  $>0.03$  mS/cm<sup>2</sup> drove the isolated dendritic compartment to depolarization block of the calcium oscillation. In the coupled model, the fast oscillation of the dendrite is not visible in the membrane potential of either compartment. However, over the range of AMPA conductances that allowed dendritic oscillation in the isolated dendrite (0–0.03 mS/cm<sup>2</sup>), the amplitude of the dendritic oscillation is at its greatest. The amplitude of the oscillation in the dendrite decreases steeply over this range as it did in the isolated compartment (Fig. 6A). The frequency of the coupled system increases slightly over a wide range of AMPA conductances (Fig. 6A). At all levels of AMPA conductance, the somatic frequency dominates the coupled system (as in Fig. 6B). The effect of the slow somatic membrane potential on the dendrite is illustrated by drawing the phase plane for the dendritic compartment, as shown in Fig. 6C. Because of voltage coupling from the relatively slow somatic oscillation, it is accurate to represent the voltage nullclines of the fast compartment as a family of curves, one for every voltage visited by the soma during its oscillation. Three such nullclines are shown in Fig. 6C, one when the soma is at its most positive voltage (–20 mV), one at the soma's negative extreme (–70 mV), and one

near the center of the somatic membrane potential trajectory (–50 mV). At all times during the cycle, the dendrite's oscillation is blocked, and the dendrite's trajectory stays close to the calcium nullcline. When the soma is hyperpolarized between spikes, its hyperpolarization is strong enough to drive the dendrite to hyperpolarization block, despite AMPA activation, and when the dendrite is released by somatic depolarization, it is driven to depolarization block of calcium oscillations by AMPA receptors. As a result, the dendrites passively follow the somatic oscillation. This was typical for AMPA activation or current injection into the dendrites for a wide range of parameters.

NMDA activation of the dendritic compartment in the same coupled configuration produced a very different result, shown in Fig. 7. Three different kinds of outcomes were observed, depending on the strength of NMDA activation. At low levels of NMDA input to the dendrites (region labeled 1 in Fig. 7, *A* and *B*), there was little change in the amplitude or frequency of the oscillation. In the uncoupled dendrite, this is the range of NMDA activations associated with the rapid increase in amplitude and frequency of dendritic oscillations. In that range, the slow oscillation at the soma continued to dominate the coupled system, and the oscillations resembled those seen during spontaneous firing. At higher levels of NMDA (region 2 in Fig. 7, *A* and *B*), the slow oscillation continued, but during the slow depolarizing phase of the oscillation, the dendrite and soma expressed a high-frequency oscillation (Fig. 7C). The

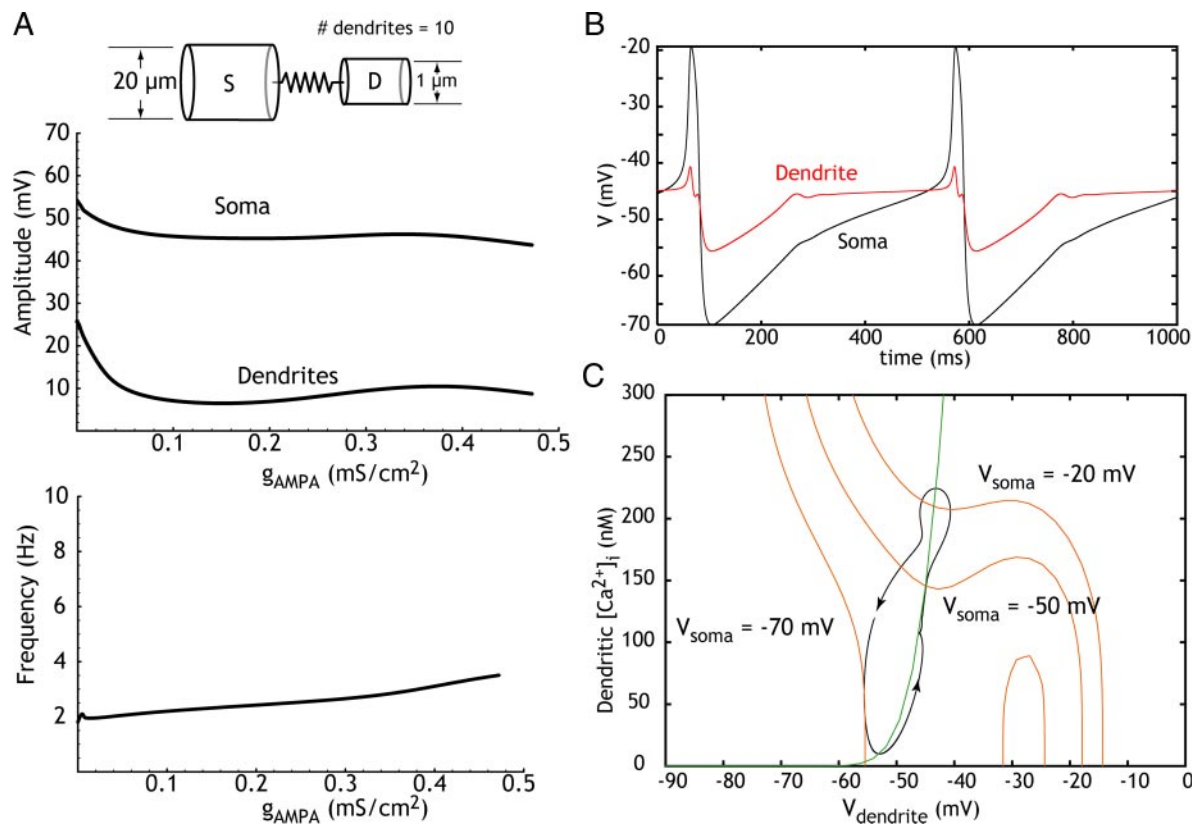


FIG. 6. AMPA activation applied to the dendrite of the 2-compartment model. *A*: amplitude and frequency of the membrane potential oscillation in the soma and dendrite with increasing AMPA activation. The dendrite undergoes rapid reduction in oscillation amplitude and subsequent voltage block of its own oscillatory mechanism over a narrow low range of conductances ( $<0.1 mS/cm^2$ ). At higher levels of activation, the dendrite is effectively passive, and provides only a tonic current injection to the dendrite on the remainder. *B*: voltage waveform of the oscillation with  $0.25 mS/cm^2$  AMPA activation. The dendritic waveform mostly mimics the somatic one. *C*: phase plane for the dendrite is shown for 3 different points during the oscillation. As the soma oscillates, the current applied to the dendrite by the soma distorts the phase space of the dendrite on a time scale slower than the dendrite's natural time scale. Thus the voltage of the soma can be treated as a slowly changing parameter. The trajectory of the dendrite stays close to the calcium nullcline, while tracking the changing stable equilibrium imposed by the soma.

higher-frequency oscillation increased in frequency and decreased in amplitude toward the end of the burst. The amplitude relationship between dendrite and soma were reversed for the two rhythms, the somatic amplitude being larger for the slow oscillation and the dendritic amplitude larger for the fast one. The amplitude of the faster oscillation grew with increases in NMDA activation, but its mean frequency was greatest at the lowest levels of activation (Fig. 7*B*). Such mixed fast-slow oscillation was observed over the range of NMDA activations labeled 2 in Fig. 7, *A* and *B*. Mixed oscillations in the coupled system were seen at levels of NMDA activation that began to produce large-amplitude oscillations in the isolated dendritic compartment (Fig. 5*B*). With higher NMDA activations (region 3 in Fig. 7), the slow oscillation was lost, and the dendrite and soma both oscillated at high frequency with the dendritic amplitude exceeding the somatic one (Fig. 7*D*). The oscillation frequency in this range decreased with additional NMDA input but remained higher than ever seen for an isolated compartment with NMDA activation and was comparable to that seen during NMDA-evoked bursts of activity in dopaminergic cells in slices and reward-related firing *in vivo*.

The mechanism of the mixed oscillations is illustrated in Fig. 7*E*. Again, the slow changes in voltage imposed on the dendrite by the soma are indicated by drawing nullclines for

the dendrite at three different somatic voltages, the extrema and the midpoint of the somatic oscillation. At the most hyperpolarized part of the somatic oscillation, the dendritic oscillation is stopped, the dendrite exhibits a stable hyperpolarized fixed point, and the dendritic trajectory approaches that fixed point. As the soma depolarizes, the dendritic voltage nullcline shifts up, and the dendritic compartment becomes unstable and oscillates. With additional upward shift of the voltage nullcline, the dendritic oscillations become lower amplitude and higher frequency. During the brief somatic final depolarization, the dendrite is driven briefly to depolarization block and then makes a final small cycle of its fast oscillation before the dendritic oscillation is abolished by the abrupt somatic hyperpolarization. This pattern characterized all the oscillations seen in region 2 of Fig. 7, *A* and *B*.

The mechanism of the fast sustained oscillations seen in region 3 and in Fig. 7*D* is shown in Fig. 7*F*. This pattern of oscillation is dominated by the dendrite, the oscillations of which are more rapid than the somatic oscillatory mechanism can follow. Effectively, the dendrite acts as a constant load on the soma approximately equal to the average voltage of the dendrite. The somatic nullclines that would apply if the dendritic voltage were fixed at the average of their oscillation are shown superimposed on the somatic trajectory in Fig. 7*F*. The

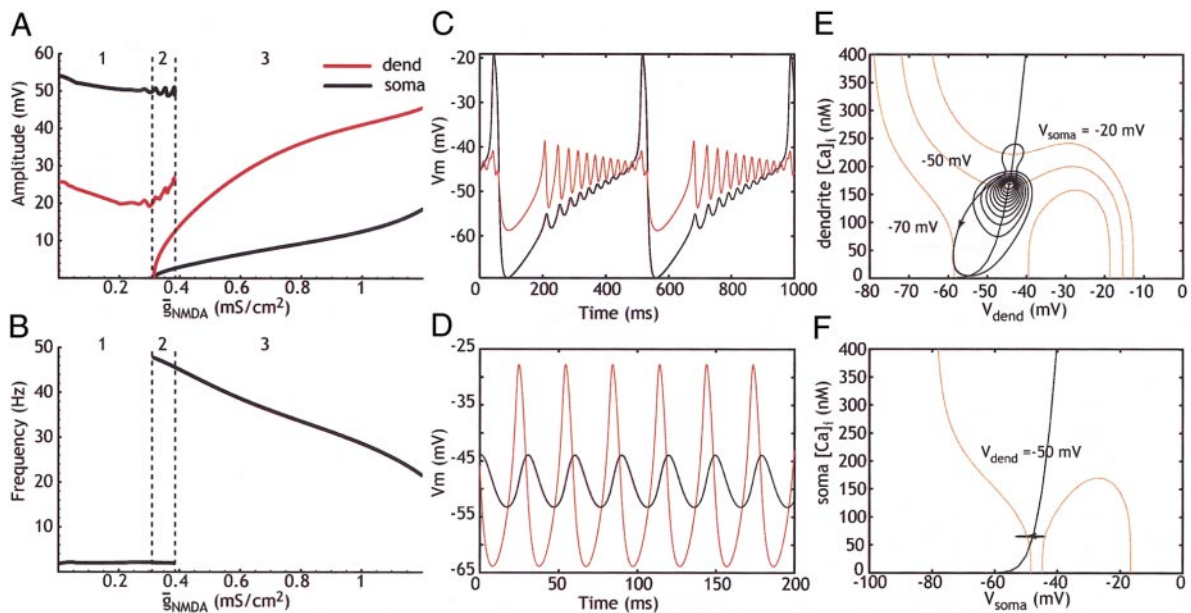


FIG. 7. Effect of dendritic NMDA activation on the 2-compartment model (number of dendrites = 10, soma diameter = 20  $\mu\text{m}$ , dendrite diameter = 1  $\mu\text{m}$ ). *A*: increasing NMDA receptor activation produces 3 qualitatively different patterns of oscillation. At low levels (region 1), amplitude of the dendritic oscillation increases slightly and frequency is almost unaffected. With small additional increases in NMDA activation, the cell exhibits low-amplitude bursting in the dendrite, which is superimposed on the slow, large-amplitude oscillation (region 2). The amplitudes and frequencies of both the slow and fast oscillation are shown in *A* and *B* for this pattern. The fast oscillation is larger in the dendrite, and the slow 1 in the soma. At higher levels of NMDA activation (region 3), the slow oscillation disappears, and the fast oscillation becomes constant (not bursting) and remains larger in the dendrite. In this region, increases in NMDA activation produce an increase in amplitude and a decrease in the frequency of the oscillation. The frequency of oscillation in region 2 is between 20 and 40 Hz. *C*: voltage waveform for the soma (black) and dendrite (red) for oscillations in region 2. *D*: voltage waveforms for the soma (black) and dendrite (red) for oscillations in region 3. Note change in time scale. *E*: phase plane trajectory for the dendrite during bursting in region 2. Voltage nullclines are drawn for various phases of the oscillation as indicated by the somatic membrane potential. Note that the dendrite is passive during the hyperpolarizing phase of the slow oscillation, but its oscillation is released from soma-imposed hyperpolarization block during the bursting phase of the cycle. *F*: phase plane trajectory for the soma during the oscillation in region 3. Note that the dendritic oscillation blocks the soma because the average dendritic voltage is hyperpolarized enough to drive the soma to hyperpolarization block through most of the cycle. Somatic depolarization occurs rapidly enough to respond during the release from hyperpolarization imposed by the dendrite, but somatic calcium cannot change concentration fast enough to respond to the rapid oscillation rate of the dendrite, and so the somatic calcium level remains low and nearly constant.

net effect of the dendritic oscillation is a hyperpolarization of the soma that blocks the somatic oscillation. The oscillation of the dendrite is passively conducted to the soma and is responsible for the small changes in voltage seen in Fig. 7*F*. Because the somatic calcium concentration cannot follow the high frequency of the driving oscillation from the dendrite, somatic calcium stays at a point determined by the average voltage nullcline and the somatic voltage follows the dendritic oscillation but with reduced amplitude and a phase shift caused by the somatic capacitance. The soma maintains a constant low calcium concentration and very little calcium-dependent potassium current. The soma exerts a small constant depolarizing influence on the dendrite, and it is the combination of somatic depolarizing current and NMDA receptor activation that drives the dendrite to high-amplitude, high-frequency oscillations. This phenomenon, in which coupled oscillators exhibit widely different amplitude, is known as localization and has been studied in a variety of contexts (e.g., Kuske and Erneux 1997; Rotstein et al. 2003). In the dopaminergic cell model, as well as in others (Rotstein et al. 2003), the results depend strongly on the strength and symmetry of the coupling.

With increases in the coupling parameter, or with reduction of the difference in diameters of the soma and dendritic compartments, application of low NMDA conductances to the dendrite could stabilize both soma and dendrite, causing re-

gions 1 and 2 in Fig. 7 to be separated by a region of stable resting potential (not shown). This occurred because each compartment shifted the voltage nullcline of the other to a position with a stable equilibrium. The interaction between coupled oscillatory compartments depends on the strength of coupling between them, the sensitivity of the oscillation to shifts in the voltage nullcline (how far each compartment is from hyperpolarization block), and the asymmetry of the effective coupling.

The results shown in Fig. 7 suggests that brief periods of NMDA activation in the dendrite might be capable of creating brief bursts of oscillatory activity in the dendrites and somata, which could trigger bursts of action potentials. The critical issue is whether the coupled system could shift from pattern 1 to pattern 3 firing and back rapidly. Such rapid shifts do occur with very little aftereffect, as demonstrated in Fig. 8, for a pair of spiking compartments as in Fig. 3. In Fig. 8*A*, a 500-ms application of NMDA to the dendrites produces a period of high-frequency oscillation superimposed on the slow spontaneous regular spiking. The dendrite and soma both fire action potentials during both the slow and fast oscillations, but the roles of the two compartments are different in the two patterns. Note that there is minimal buildup of somatic calcium during the burst despite the high-frequency oscillations, as in the phase plane of Fig. 7*F*, and after the burst, the cell returns to its resting oscillation with very little delay. Because individual

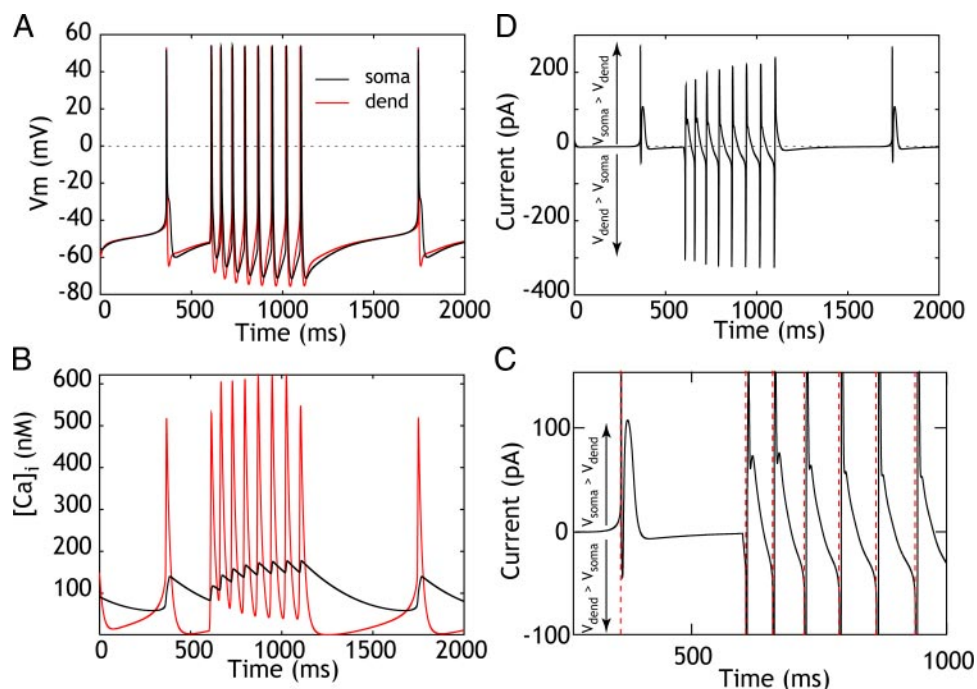


FIG. 8. NMDA-induced bursting in the 2-compartment ( $10 \times 1 \mu\text{m}$  dendrites,  $20 \mu\text{m}$  soma) spiking model used in Fig. 3. NMDA ( $0.4 \text{ mS/cm}^2$ ) is applied for 500 ms starting at 600 ms. *A*: The background firing rate is slow, and is dominated by the soma. During the application of NMDA, firing rapidly increases to  $< 20 \text{ Hz}$ . *B*: During the rapid firing, somatic calcium increases slowly with each action potential contributing much less calcium increase than that seen during spontaneous firing. Dendritic calcium transients remain large throughout high-frequency firing. *C*: Current passing between soma and dendrite during the firing in *A* and *B*. The mechanism of rapid firing is a switch from soma-dominated oscillation to dendritic oscillation. During the slow oscillation, somatic depolarization leads dendritic at the threshold of firing, and action potentials originate in the soma. This is indicated by the large amplitude fast positive current pulse at the beginning of each spontaneous oscillation. The dendrite is primarily responsible for the rapid repolarization following the action potential. During the burst, dendritic depolarization leads during spike initiation and the dendrite fires first, as indicated by the large downward transients. *D*: Expanded view of currents associated with spontaneous (left) and bursting (right) spikes. Time of onset of spikes is indicated by red dashed lines. Parameters as in Table 1, except  $\bar{g}_{\text{ca}} = 0.15 \text{ ms/cm}^2$ ,  $g_{\text{c}} = 30 \text{ nS/cm}^2$ .

action potentials do not generate large calcium concentration changes in dopaminergic neurons, the rapid action potentials do not result in a large calcium transient, and the cell resumes its slow oscillation after only a brief period following the burst.

The mechanism responsible for the burst is similar to that for the nonspiking two-compartment system in that it relies on oscillation generated by subthreshold currents. During spontaneous firing, the somatic natural frequency of oscillation dominates, and action potentials are generated initially in the soma and subsequently in the dendrites. The dendrite is held in hyperpolarization block throughout much of the cycle, but its oscillation is released only briefly at the time of the action potential. Calcium-dependent potassium current in the dendrite provides much of the early afterhyperpolarization current at the soma. During application of NMDA, the roles of the dendrite and soma are reversed, as can be seen from the longitudinal current flowing between compartments (Fig. 8, *C* and *D*). The fast calcium oscillation of the dendrite is increased by NMDA activation. During the fast oscillation, action potentials are initiated in the dendrite and propagate to the soma. Although the average effect of the dendrite on the soma is hyperpolarizing (as it was for the nonspiking model), some calcium accumulation does occur in the soma due to calcium current activation during action potential generation. It is critical that the powerful calcium-dependent potassium current in the dendrite produces the hyperpolarization of the soma required to remove sodium inactivation and to enable a subsequent action

potential (Fig. 8*D*). The dendrite then immediately depolarizes again and initiates another action potential. Because the oscillation is primarily generated on the faster time scale of the dendrite, its onset and offset are rapid and have little influence on the somatic calcium concentration.

#### DISCUSSION

The dopaminergic neurons of the substantia nigra (and ventral tegmental area) are among the few cell types whose activity has been seen to correspond to clearly defined psychological states in animals (Dayan and Balleine 2002; Hyland et al. 2002; Schultz 2002), exhibiting brief episodes of high-frequency firing, or brief pauses, corresponding to changes in reward expectation. These changes in firing rate are superimposed on a  $< 10/\text{s}$  background-firing rate, which is essential if the neuron is to be able to signal reward expectation error in both directions (Tobler et al. 2003). Although this finding is exciting, it is puzzling because it seems to endow the dopaminergic neuron with the ability to use sensory inputs and past experience to predict reward. How can the dopaminergic cell gain access to this information? Possibly, the dopaminergic cell only relays this signal, which may be generated elsewhere. Or perhaps only components of the information required are present in any one class of the various inputs to the dopaminergic cell, and the overall signal must be synthesized by the neuron from those components. The search for the afferents

that inform the firing of dopaminergic cells may be guided by a knowledge of the cellular-level properties of the dopaminergic neuron that determine its response to synaptic inputs. Thus the cellular mechanisms of firing of the dopaminergic cell have been the subject of intense study during the past 20 yr.

#### *Bursting requires a synaptic trigger*

Starting with the pioneering *in vivo* intracellular recordings of Grace and Bunney (1984a, 1984b), the rhythmic, background firing of the dopaminergic neuron has been recognized as arising from an autonomous pacemaker mechanism. Subsequent studies have identified the specific ion channels responsible for pacemaking in this neuron (Fujimura and Matsuda 1989; Grace and Onn 1989; Harris et al. 1989; Kang and Kitai 1993a,b; Kita et al. 1986; Mercuri et al. 1994; Nedergaard et al. 1993; Shepard and Bunney 1991; Wolfart and Roeper 2002; Wolfart et al. 2001; Yung et al. 1991). Building on the identification of ion channels responsible for that mechanism, there have been several computational models that have examined the interactions among ion channels that give rise to the subthreshold mechanisms responsible for pacemaking (Amini et al. 1999; Li et al. 1996; Wilson and Callaway 2000). The mechanisms responsible for the irregular pattern of firing often seen *in vivo* (Hyland et al. 2002; Tepper et al. 1995; Wilson et al. 1977) are less clear. Presumably, the irregular firing pattern requires synaptic mechanisms because it is not seen in slices. However, this does not rule out constitutive properties of the dopaminergic cell that might generate irregularities in firing in the presence of synaptic influences (Canavier et al. 2004; Rodriguez et al. 2003).

Irregular and rhythmic firing are not discrete states of the dopaminergic neuron. Some indication of the single spike pacemaker responsible for rhythmic firing is apparent in the firing patterns of cells firing irregularly (Rodriguez et al. 2003; Wilson et al. 1977). By convention, any pattern that includes bursts *in vivo* is called a bursting pattern, but bursts in dopaminergic neurons are actually singular events superimposed on the rhythmic or irregular single spiking pattern (Grace and Bunney 1984a; Hyland 2002; Tepper et al. 1995). In awake animals, bursts are associated with very specific behavioral circumstances (Hyland 2002; Schultz 2002) and so must be triggered by, or at least tightly controlled by, synaptic inputs. Spontaneous bursting in dopaminergic neurons in anesthetized animals does occur, and even in this preparation, bursts not generated rhythmically but are isolated events that are superimposed on a single-spiking pattern. Spontaneous bursts in anesthetized animals are a curiosity in any case because the behavioral conditions for burst generation are ostensibly absent. Perhaps spontaneous bursting reflects random occurrences of the same circuit events required for behaviorally significant bursting in awake animals. It is possible that spontaneous bursts arise from an entirely different mechanism. Given their relation to behavior, bursts are likely to depend on synaptic input, but it is not certain the extent to which synaptic input serves only to trigger a burst, or to guide and shape the bursts (but see Paladini and Tepper 1999).

#### *Alternative mechanisms of burst firing*

In principle, the explanation for synaptically driven bursting need not be complex. For those cells having the capacity to fire

much faster than their spontaneous rate, all that is needed is a suprathreshold depolarization of the correct duration. Synaptic excitation is a likely source of such depolarizations, and dopaminergic neurons receive excitatory glutamatergic and nicotinic cholinergic input from a number of sources (Kitai et al. 1999; Overton and Clark 1997). But in dopaminergic neurons, the precondition for this mechanism is not met. Depolarizing pulses applied to these cells via intracellular electrodes have consistently failed to drive firing that resembles natural bursts either in pattern or in rate (Grace and Bunney 1983a; Kang and Kitai 1993a; Kita et al. 1986; Richards et al. 1997). Firing in response to modest current pulses that allow repetitive firing never achieves the high rates observed in natural bursts. When driven with currents in excess of those required to get above the maximum spontaneous rate (4–10 Hz), firing of dopaminergic cells fails rapidly, apparently due to depolarization block of the spiking currents (Richards et al. 1997). Application of excitatory neurotransmitters, such as nicotinic cholinergic agonists (Grillner and Mercuri 2002; Sorenson et al. 1998), or AMPA agonists (Chergui et al. 1993; Johnson et al. 1992), likewise can produce increases in firing rate but do not drive the cells to fire at the >10 Hz rates commonly seen during *in vivo* bursts.

Because the firing rate of the dopaminergic neuron is limited by the prominent afterhyperpolarization that follows each spike during rhythmic spontaneous spiking, one class of possible alternative mechanisms could arise from suppression of the calcium dependent potassium current that is responsible for the afterhyperpolarization (Ping and Shepard 1996; Shepard and Bunney 1991). Spiking in dopaminergic neurons treated with apamin (to block this current) is fragile, however, and can trigger large plateau depolarizations that rapidly lead to spike failure. Sustained spiking can occur only in a narrow range of potentials in which the cell is depolarized sufficiently to maintain sustained firing but does not undergo depolarization block (Johnson and Wu 2004; Shepard and Bunney 1991). Identification of a synaptic mechanism with an apamin-like effect on the AHP sufficient to generate bursts has not been successful, although SK-induced current has been shown to be reduced somewhat by NMDA activation and by muscarinic cholinergic agonists (Kitai et al. 1999; Paul et al. 2003).

The calcium channels underlying subthreshold membrane potential oscillations are mostly responsible for calcium-dependent  $K^+$  current in dopaminergic cells. The presence or absence of an action potential superimposed on these oscillations does not have a large effect on calcium influx or on the amplitude or duration of the hyperpolarizing phase of the subthreshold oscillation, which is primarily due to SK channels (Kang and Futami 1999; Wilson and Callaway 2000). The absence of a big contribution from fast action potentials is apparently due to the low threshold of voltage-sensitive calcium channels responsible for the AHP (Kang and Kitai 1993a; Wilson and Callaway 2000; Wolfart and Roeper 2002). It is probably also the reason the firing pattern that results of SK blockade does not greatly resemble the bursting seen *in vivo* but consists primarily of an alteration of the subthreshold oscillation, characterized by long-duration plateau potentials that trigger a few spikes at the beginning before the spike fails because of depolarization block of the spike.

### *NMDA receptor activation is specifically associated with bursting*

A number of studies suggest that NMDA receptor activation may play a crucial role in generating bursts in dopaminergic cells *in vivo*. Dopaminergic neurons express NMDA receptors on their somata and dendrites (Albers et al. 1999; Lin and Lipski 2001; Paquet et al. 1997). Application of NMDA antagonists to dopaminergic cells *in vivo* regularizes their firing and abolishes spontaneous bursting, which effect is not shared by non-NMDA glutamate antagonists (Chergui et al. 1993; Overton and Clark 1993). Bursting can also be evoked by stimulation of cortical regions with direct or indirect synaptic connections with dopaminergic neurons, and that bursting is also suppressed by NMDA antagonists (Tong et al. 1996). It is especially interesting that in these experiments the effective antagonists did not block the excitatory response to stimulation completely, but only the bursts. Bursts can also be evoked *in vivo* by stimulation of other structures contributing glutamatergic inputs to the substantia nigra, particularly the pedunculopontine nucleus (Lokwan et al. 1999) and the subthalamic nucleus (Smith and Grace 1992).

NMDA receptor activation can also produce burst firing of dopaminergic neurons in slices. Bath application of NMDA and NMDA antagonists has been studied the most and has been one of the principal models for bursting in dopaminergic cells (Amini et al. 1999; Canavier 1999; Johnson and Wu 2004; Johnson et al. 1992; Li et al. 1996). Bath application of NMDA to slices can induce rhythmic plateau potentials in dopaminergic neurons especially if combined with blockade of SK channels or intracellular calcium chelation (Johnson and Wu 2004). The mechanism of these plateau potentials is apparently connected to dendritic sodium disposition and has been the subject of extensive examination, both experimentally and theoretically (Canavier 1999; Johnson et al. 1992; Li et al. 1996; Shen and Johnson 1998). Even in the absence of apamin or other treatment that could reduce the AHP, about one-third of dopaminergic neurons in slices exhibit spontaneous bursting on treatment with 10 mM NMDA (Johnson and Wu 2004). As with apamin treatment, bath application of NMDA agonists produces rhythmically occurring plateau potentials that do not resemble bursts as seen *in vivo*. However, this treatment can evoke high-frequency firing (in excess of the 10-Hz limit for background and driven firing). Perhaps the *in vivo* burst is caused by a brief period of NMDA activation, insufficient to produce rhythmic plateau potentials but long enough to evoke a single burst.

In support of this view, bursting can be elicited by direct iontophoretic application of glutamate or NMDA to dendrites of dopaminergic cells or stimulation of glutamatergic afferents to the dendrites of dopaminergic neuron (Morikawa et al. 2003). Bursts of firing at  $>10/s$  could be evoked by synaptic stimulation or applied aspartate and were shown to be dependent on activation of NMDA receptors. Bursts happened in the absence of any plateau potential and resembled natural bursts in appearance. They were followed by a long-duration pause in firing, which was blocked by antagonists of metabotropic glutamate receptor, which also inhibited release of calcium from intracellular stores. These results suggest that NMDA receptor activation may be the principal mechanism of bursting in dopaminergic neurons and may occur without generation of

plateau potentials. They also indicate that the pause in firing following bursts may arise from a separate cellular mechanism from the burst, explaining the absence of pauses following bursts seen in behaving animals (e.g., Schultz 2002).

### *How does NMDA receptor activation promote bursting?*

Previous models of the dopaminergic neuron have focused either on the sodium-based mechanism of NMDA-evoked rhythmic plateau potentials (Canavier 1999; Komendantov and Canavier 2001; Li et al. 1996) or on the calcium-mediated slow oscillation responsible for the background firing (Amini et al. 1999; Wilson and Callaway 2000). In the models of NMDA-induced rhythmic bursting, the main purpose was to explain the plateau potential not the high-frequency firing. High-frequency firing in those models was a simple consequence of that depolarization, and depolarizing current injections at the soma would have the same effect. Thus while these models do explain the rhythmic plateau potentials seen during bath application of NMDA, they do not account for high-frequency firing during natural bursts (or during NMDA-induced plateau potentials) given that in nature the dopaminergic neuron's action potential fails during prolonged depolarizations. For the same reason, they cannot account for the NMDA bursts seen in the Morikawa et al. (2003) study or for the dissociation between bursting and the postburst hyperpolarizations and pauses seen in that study. The model presented here does not address the sodium mechanism responsible for plateau potentials but rather the interaction between NMDA receptor activation and the calcium mechanism responsible for the slow rhythmic background firing. We have shown that the special status of NMDA in driving high-frequency firing is a natural consequence of the coupled oscillator model of the dopaminergic neurons. In this model, burst firing evoked specifically by dendritic NMDA receptor activation arises, not from a special set of ion channels, but by the same mechanism responsible for the slow single spiking oscillation. The change that is responsible for the burst is not a shift in the ion channels responsible for shaping the firing of dopaminergic neurons but the transient dominance of dendritic oscillation over that of the soma.

In the coupled oscillator model, the entire somatodendritic surface of the dopaminergic neuron possesses the mechanism responsible for rhythmic single spiking. The essential components of the mechanism are a low-threshold but mostly noninactivating calcium current, plasma membrane calcium pump, and the SK-type calcium-dependent potassium current. Other mechanisms, including intracellular calcium stores and buffers, a persistent sodium current, transient voltage-sensitive potassium currents, and hyperpolarization-activated cation current, all participate and adjust the oscillatory period of this mechanism, but the main determinant of the period of oscillation is the geometry of the neuron. Because most of the time during each cycle of the oscillation is occupied by the process of calcium filling of the cytoplasm or calcium removal, the surface area to volume ratio of each part of the cell determines the natural frequency of the oscillation at that part. Voltage coupling is strong enough (part of the time) to enforce a single oscillatory frequency across the somatodendritic membrane despite the wide variation of natural frequencies represented. During rhythmic single spiking, as seen in slices and often *in vivo*, the slow somatic membrane dominates the much faster

oscillation of the dendrites. This happens because, despite the large dendritic surface area, the fast oscillations of the dendritic membrane have a low amplitude and thus provide little current with which to counteract the large amplitude slow oscillations of the somatic compartment. Dendritic NMDA receptor activation, because of its voltage dependence, acts as a current amplifier for the dendritic oscillation. The large surface area of the dendrites can, when amplified in this way, escape control by the soma and express their high-frequency oscillation along with that of the slower one. With higher levels of NMDA activation, the dendrites may dominate the soma and suppress the slow oscillation completely. The processes responsible for this are already present in a very simple and primitive representation of the dopaminergic neuron.

The mechanism of bursting relies on this switch between somatic and dendritic subthreshold oscillations but also on the peculiar spiking behavior of dopaminergic neurons. The propensity of dopaminergic cells to depolarization block of spiking was pointed out by Grace and Bunney (1983a, 1984a) and has been noted by many others. It is visible in the low safety factor for antidromic invasion of the soma and dendrites and for the decomposition of action potentials during spontaneous and driven bursting (Grace and Bunney 1983b). On the other hand, the dopaminergic neuron also exhibits a high reliability of dendritic backpropagation of action potentials when they do invade the somatodendritic membrane, and dendrites are capable of generating action potentials (Hausser et al. 1995; Nedergaard and Hounsgaard 1996). In the model presented here, the origination point of action potentials shifted from the somatic to dendritic compartments during bursts, but both the somatic and dendritic membrane either fired or failed together. The crucial ingredient for the action potential to follow the high-frequency subthreshold oscillation generated by the dendrite was fast repolarization of the cell by the subthreshold (calcium-dependent potassium current) mechanism. In our model, the dopaminergic cell's spike mechanism is fragile, not because it has unusual sodium currents, but because the spike-generated AHP currents are not sufficient to repolarize the cell and remove sodium channel inactivation. During slow single spiking, the cell fires single spikes per cycle of the subthreshold oscillation because the fast sodium channel retains substantial inactivation after a single spike to produce an elevated threshold and prevent subsequent spiking. This sodium inactivation is removed only on the hyperpolarizing phase of the subthreshold oscillation (by the calcium-dependent K current). Thus high-frequency spiking can occur only when the cell is driven by a high-frequency subthreshold oscillation. This explains the fragility of the spiking mechanism after poisoning with apamin and the failure of the cell to fire rapidly in response to constant depolarizing currents (including those arising from AMPA and nicotinic ACh receptors). The crucial role of NMDA receptor activation comes from its ability to amplify a high-frequency dendritic oscillation that includes a powerful spike-independent repolarizing current after each action potential.

#### *Afferent control of bursting in dopaminergic cells*

Our results suggest that the synaptic inputs responsible for burst generation in dopaminergic neurons may act primarily to alter the intrinsic membrane properties responsible for sub-

threshold oscillation. This mode of synaptic action is very different from the usual formulation in which synaptic currents deposit charge on the membrane that changes the membrane potential through redistribution on the cell membrane. In the mechanism we envision, there is no need for a synaptic potential, or a graded potential that decays over time and space, and no question of whether a synapse will bring the cell closer or farther from spike threshold. Instead, the voltage-dependent synaptic current from NMDA receptors is added to the balance of currents that make up the subthreshold oscillator, increasing the contribution of the stimulated dendrite to a discrete transition between alternative intrinsic firing modes. There is still the opportunity for spatial summation among synapses. In our model, all dendritic compartments are simultaneously treated with NMDA. In a real neuron, only a subset of the dendrites may receive synaptic input at any one time. The generation of a burst will require some threshold number of dendrites activated, comparable to the parameter  $n_d$  in our model.

An intriguing feature of the mechanism we have proposed is its dependence on cell shape. The cause of the wide range of natural frequencies in our model is the discrepancy in size between the somatic and dendritic compartments. Without this, and without the differential distribution of synapses on the fine dendrites and soma, burst generation could not occur in the coupled oscillator model. In this formulation, small distal dendrites are not a less effective site for excitatory synapses in the control of firing, but on the contrary, the smallest dendrites are most advantageous for synaptic generation of bursts.

#### GRANTS

This work was supported by National Institute of Neurological Disorders and Stroke Grant NS-047085 to C. J. Wilson and National Science Foundation Grant DMS-0109427 to N. Kopell.

#### REFERENCES

- Albers DS, Weiss SW, Iadarola MJ, and Standaert DG. Immunohistochemical localization of *N*-methyl-D-aspartate and alpha-amino-3-hydroxy-5-methyl-4-isoxazolepropionate receptor subunits in the substantia nigra pars compacta of the rat. *Neuroscience* 89: 209–220, 1999.
- Amini B, Clark JW, and Canavier CC. Calcium dynamics underlying pacemaker-like burst firing oscillations in midbrain dopaminergic neurons: a computational study. *J Neurophysiol* 82: 2249–2261, 1999.
- Canavier CC. Sodium dynamics underlying burst firing and putative mechanisms for the regulation of the firing pattern in midbrain dopamine neurons: a computational approach. *J Comput Neurosci*. 6:49–69, 1999.
- Canavier CC, Perla SR, and Shepard PD. Scaling of prediction error does not confirm chaotic dynamics underlying irregular firing using interspike intervals from midbrain dopamine neurons. *Neuroscience* 129: 491–502, 2004.
- Celada P, Paladini CA, and Tepper JM. GABAergic control of rat substantia nigra dopaminergic neurons: role of globus pallidus and substantia nigra pars reticulata. *Neuroscience* 89: 813–825, 1999.
- Centonze D, Gubellini P, Pisani A, Bernardi G, and Calabresi P. Dopamine, acetylcholine and nitric oxide systems interact to induce corticostriatal synaptic plasticity. *Rev Neurosci* 14: 207–216, 2003.
- Chergui K, Charley PJ, Akaoka H, Saunier CF, Brunet, J.-L., Buda M, Svensson TH, and Chovet G. Tonic activation of NMDA receptors causes spontaneous burst discharge of rat midbrain dopamine neurons in vivo. *Eur J Neurosci* 5:137–144, 1993.
- Dayan P and Balleine BW. Reward, motivation and reinforcement learning. *Neuron* 36: 285–298, 2002.
- Durante P, Cardenas CG, Whittaker JA, Kitai ST, and Scroggs RS. Low-threshold L-type calcium channels in rat dopaminergic neurons. *J Neurophysiol* 91: 1450–1454, 2004.
- Ermentrout B. *Simulating, Analyzing, and Animating Dynamical Systems: A Guide To Xppaut for Researchers and Students*. Philadelphia, PA: Society for Industrial and Applied Mathematics, 2002.

- Fujimura K and Matsuda Y.** Autogenous oscillatory potentials in neurons of the guinea pig substantia nigra pars compacta in vitro. *Neurosci Lett* 104: 53–57, 1989.
- Grace AA and Bunney BS.** Intracellular and extracellular electrophysiology of nigral dopaminergic neurons. I. Identification and characterization. *Neuroscience* 10: 301–315, 1983a.
- Grace AA and Bunney BS.** Intracellular and extracellular electrophysiology of nigral dopaminergic neurons. II. Action potential generating mechanisms and morphological correlates. *Neuroscience* 10: 317–331, 1983b.
- Grace AA and Bunney BS.** The control of firing pattern in nigral dopamine neurons: single spike firing. *J Neurosci* 4: 2866–2876, 1984a.
- Grace AA and Bunney BS.** The control of firing pattern in nigral dopamine neurons: burst firing. *J Neurosci* 4: 2877–2890, 1984b.
- Grace AA and Onn, S.-P.** Morphology and electrophysiological properties of immunocytochemically identified rat dopamine neurons recorded in vitro. *J Neurosci* 9: 3463–3481, 1989.
- Grillner P and Mercuri NB.** Intrinsic membrane properties and synaptic inputs regulating the firing activity of the dopamine neurons. *Behav Brain Res* 130:149–169, 2002.
- Harris NC, Webb C, and Greenfield SA.** A possible pacemaker mechanism in pars compacta neurons of the guinea pig substantia nigra revealed by various ion channel blocking agents. *Neurosci*. 31: 355–362, 1989.
- Hausser M, Stuart G, Racca C, and Sakmann B.** Axonal initiation and active dendritic propagation of action potentials in substantia nigra neurons. *Neuron* 15: 637–647, 1995.
- Hyland BI, Reynolds JNJ, Hay J, Perk CG, and Miller R.** Firing modes of midbrain dopamine cells in the freely moving rat. *Neuroscience* 114: 475–492, 2002.
- Johnson SW, Seutin V, and North RA.** Burst firing in dopamine neurons induced by *N*-methyl-D-aspartate: role of electrogenic sodium pump. *Science* 258: 655–657, 1992.
- Johnson SW and Wu Y-N.** Multiple mechanisms underlie burst firing in rat midbrain dopamine neurons in vitro. *Brain Res* 1019: 293–296, 2004.
- Juraska JM, Wilson CJ, and Groves PM.** The substantia nigra of the rat: a Golgi study. *J Comp Neurol* 172: 585–600, 1977.
- Kang Y and Futami T.** Arrhythmic firing in dopamine neurons of rat substantia nigra evoked by activation of subthalamic neurons. *J Neurophysiol* 82: 1632–1637, 1999.
- Kang Y and Kitai ST.** A whole cell patch-clamp study on the pacemaker potential in dopaminergic neurons of rat substantia nigra compacta. *Neurosci Res* 18: 209–221, 1993a.
- Kang Y and Kitai ST.** Calcium spike underlying rhythmic firing in dopaminergic neurons of the rat substantia nigra. *Neurosci Res* 18:195–207, 1993b.
- Kita T, Kita H, and Kitai ST.** Electrical membrane properties of rat substantia nigra compacta neurons in an in vitro slice preparation. *Brain Res* 372: 21–30, 1986.
- Kitai ST, Shepard PD, Callaway JC, and Scroggs R.** Afferent modulation of dopamine neuron firing patterns. *Curr Opin Neurobiol* 9: 690–697, 1999.
- Kiyatkin EA and Rebec GV.** Heterogeneity of ventral tegmental area neurons: single-unit recording and iontophoresis in awake, unrestrained rats. *Neuroscience* 85: 1285–1309, 1998.
- Komendantov AO and Canavier CC.** Electrical coupling between model midbrain dopamine neurons: effects on firing pattern and synchrony. *J Neurophysiol* 87: 1526–1541, 2002.
- Komendantov AO, Komendantova OG, Johnson SW, and Canavier CC.** A modeling study suggests complementary roles for GABA<sub>A</sub> and NMDA receptors and the SK channel in regulating the firing pattern in midbrain dopamine neurons. *J Neurophysiol* 91: 346–357, 2004.
- Kuske R and Erneaux T.** Localized synchronization of two coupled solid state lasers. *Optical Commun* 139: 125–131, 1997.
- Lacey MG, Mercuri NB, and North RA.** Two cell types in rat substantia nigra zona compacta distinguished by membrane properties and the action of dopamine and opioids. *J Neurosci* 8: 1233–1241, 1987.
- Li Y-X, Bertram R, and Rinzel J.** Modeling *N*-methyl-D-aspartate-induced bursting in dopamine neurons. *Neuroscience* 71: 397–410, 1996.
- Lin JY and Lipski J.** Dopaminergic substantia nigra neurons express functional NMDA receptors in postnatal rats. *J Neurophysiol* 85: 1336–1339, 2001.
- Lokwan SJA, Overton PG, Berry MS, and Clark D.** Stimulation of the pedunculopontine tegmental nucleus in the rat produces burst firing in A9 dopaminergic neurons. *Neuroscience* 92: 245–254, 1999.
- Mayer ML and Westbrook GL.** The action of *N*-methyl-D-aspartic acid on mouse spinal neurons in culture. *J Physiol* 361: 65–90, 1985.
- Medvedev GS and Kopell N.** Synchronization and transient dynamics in chains of electrically coupled FitzHugh-Nagumo oscillations. *SIAM J Appl Math* 61: 1763–1801, 2001.
- Medvedev GS, Wilson CJ, Callaway JC, and Kopell N.** Dendritic synchrony and transient dynamics in a coupled oscillator model of the dopaminergic neuron. *J Comput Neurosci* 15: 53–69, 2003.
- Mercuri NB, Bonci A, Calabresi, P. Stratta F, Stefani A, and Bernardi G.** Effects of dihydropyridine calcium antagonists on rat midbrain dopaminergic neurones. *Br J Pharmacol* 113: 831–838, 1994.
- Morikawa H, Khodakhah K, and Williams JT.** Two intracellular pathways mediate metabotropic glutamate receptor-induced Ca<sup>2+</sup> mobilization in dopamine neurons. *J Neurosci* 23: 149–157, 2003.
- Nedergaard S.** A Ca<sup>2+</sup>-independent slow afterhyperpolarization in substantia nigra compacta neurons. *Neuroscience* 125: 841–852, 2004.
- Nedergaard S, Flatman JA, and Engberg I.** Nifedipine- and omega-conotoxin-sensitive Ca<sup>2+</sup> conductances in guinea pig substantia nigra pars compacta neurones. *J Physiol* 466: 727–747, 1993.
- Nedergaard S and Greenfield SA.** Sub-populations of pars compacta neurons in the substantia nigra: the significance of qualitatively and quantitatively distinct conductances. *Neuroscience* 48: 423–437, 1992.
- Nedergaard S and Hounsgaard J.** Fast Na<sup>+</sup> spike generation in dendrites of guinea pig substantia nigra pars compacta neurons. *Neuroscience* 73: 381–396, 1996.
- Neuhoff H, Neu A, Liss B, and Roeper J.** Ih channels contribute to the different functional properties of identified dopaminergic subpopulations in the midbrain. *J Neurosci* 22: 1290–1302, 2002.
- Nicola SM, Surmeier J, and Malenka RC.** Dopaminergic modulation of neuronal excitability in the striatum and nucleus accumbens. *Annu Rev Neurosci* 23: 185–215, 2000.
- Overton P and Clark D.** Iontophoretically administered drugs acting at the *N*-methyl-D-aspartate receptor modulate burst firing in A9 dopamine neurons in the rat. *Synapse* 10: 131–140, 1993.
- Overton PG and Clark D.** Burst firing in midbrain dopaminergic neurons. *Brain Res Rev* 25: 312–334, 1997.
- Paladini CA and Tepper JM.** GABA<sub>A</sub> and GABA<sub>B</sub> antagonists differentially affect the firing pattern of substantia nigra dopaminergic neurons in vivo. *Synapse* 32: 165–176, 1999.
- Paquet M, Tremblay M, Soghomonian JJ, and Smith Y.** AMPA and NMDA glutamate receptor subunits in midbrain dopaminergic neurons in the squirrel monkey: an immunohistochemical and in situ hybridization study. *J Neurosci* 17: 1377–1396, 1997.
- Paul K, Keith DJ, and Johnson SW.** Modulation of calcium-activated potassium small conductance (SK) current in rat dopamine neurons of the ventral tegmental area. *Neurosci Lett* 2003 348: 180–184, 2003.
- Ping HX and Shepard PD.** Apamin-sensitive Ca(2+)-activated K<sup>+</sup> channels regulate pacemaker activity in nigral dopamine neurons. *Neuroreport* 7: 809–814, 1996.
- Richards CD, Shiroyama T, and Kitai ST.** Electrophysiological and immunocytochemical characteristics of GABA and dopamine neurons in the substantia nigra of the rat. *Neuroscience* 80: 545–557, 1997.
- Rodriguez M, Pereda E, Gonzalez J, Abdala P, and Obeso JA.** How is firing activity of substantia nigra cells regulated? Relevance of pattern-code in the basal ganglia. *Synapse* 49: 216–225, 2003.
- Rotstein HG, Kopell N, Zhabotinsky AM, and Epstein IR.** A canard mechanism for localization in systems of globally coupled oscillators. *SIAM J Appl Math* 63: 1998–2019, 2003.
- Schultz W.** Getting formal with dopamine and reward. *Neuron* 36: 241–263, 2002.
- Shen K-Z and Johnson SW.** Sodium pump evokes high density pump currents in rat midbrain dopamine neurons. *J Physiol* 512: 449–457, 1998.
- Shepard PD and Bunney BS.** Repetitive firing properties of putative dopamine-containing neurons in vitro: regulation by an apamin-sensitive Ca(2+)-activated K<sup>+</sup> conductance. *Exp Brain Res* 86: 141–150, 1991.
- Smith ID and Grace AA.** Role of the subthalamic nucleus in the regulation of nigral dopamine neuron activity. *Synapse* 12: 287–303, 1992.
- Sorenson EM, Shiroyama T, and Kitai ST.** Postsynaptic nicotinic receptors on dopaminergic neurons in the substantia nigra pars compacta of the rat. *Neuroscience* 87: 659–673, 1998.
- Tepper JM, Martin LP, and Anderson DR.** GABA<sub>A</sub> receptor-mediated inhibition of rat substantia nigra dopaminergic neurons by pars reticulata projection neurons. *J Neurosci* 15: 3092–3103, 1995.
- Tepper JM, Sawyer SF, and Groves PM.** Electrophysiologically identified nigral dopaminergic neurons intracellularly labeled with HRP: light-microscopic analysis. *J Neurosci* 7: 2794–2806, 1987.



- Tobler PN, Dickinson A, and Schultz W.** Coding of predicted reward omission by dopamine neurons in a conditioned inhibition paradigm. *J Neurosci* 23: 10402–10410, 2003.
- Tong ZY, Overton PG, and Clark D.** Antagonism of NMDA receptors but not AMPA/kainate receptors blocks bursting in dopaminergic neurons induced by stimulation of the prefrontal cortex. *J Neural Transm* 103: 889–904, 1996.
- Wilson CJ and Callaway JC.** A coupled oscillator model of the dopaminergic neuron of the substantia nigra. *J Neurophysiol* 83: 3084–3100, 2000.
- Wilson CJ, Young SJ, and Groves PM.** Statistical properties of neuronal spike trains in the substantia nigra: Cell types and their interactions. *Brain Res* 136: 243–260, 1977.
- Wolfart J, Neuhoff H, Franz O, and Roeper J.** Differential expression of the small-conductance, calcium-activated potassium channel SK2 is critical for pacemaker control in dopaminergic midbrain neurons. *J Neurosci* 21: 3443–3456, 2001.
- Wolfart J and Roeper J.** Selective coupling of T-type calcium channels to SK potassium channels prevents intrinsic bursting in dopaminergic midbrain neurons. *J Neurosci* 22: 3404–3413, 2002.
- Yung WH, Hausser MA, and Jack JJ.** Electrophysiology of dopaminergic and non-dopaminergic neurons of the guinea pig substantia nigra pars compacta in vitro. *J Physiol* 436: 643–667, 1991.